A Model for Mechanical Property Evaluation of the Periodic Porous Low-k Materials by SAW*

Li Zhiguo, Yao Suying, Xiao Xia†, and Bai Maosen

(*ASIC Design Center, School of Electronic and Information Engineering, Tianjin University, Tianjin 300072, China*)

Abstract: The influence of the distribution of nano-pores on the mechanical properties evaluation of porous low-k films by surface acoustic waves (SAW) is studied. A theoretical SAW propagation model is set up to characterize the periodic porous dielectrics by transversely isotropic symmetry. The theoretical deductions of SAW propagating in the low-k film/Si substrate layered structure are given in detail. The dispersive characteristics of SAW in different propagation directions and the effects of the Young's moduli E, E' and shear modulus G' of the films on these dispersive curves are found. Computational results show that E' and G' cannot be measured along the propagation direction that is perpendicular to the nano-pores' direction.

Key words: periodic porous materials; low-k dielectrics; transversely isotropic symmetry; mechanical property; SAW measurement

PACC: 0340K; 0630M; 6860 **EEACC**: 2570; 2800; 7320G

CLC number: TN405.97 **Document code**: A **Article ID**: 0253-4177(2007)11-1722-07

1 Introduction

To minimize signal propagation delay, crosstalk noise, and power consumption, it is critical for ULSI interconnect systems to develop low dielectric constant (k) materials that are integrated with Cu meta[1]. Because it is difficult to reduce the k value below 2.0 with dense materials, the introduction of nano-pores into the dielectrics seems inevitable to achieve ultra low-k materials[2]. Porous low-k material should have sufficient mechanical, chemical, and thermal qualities to survive integration processes, such as chemical mechanical polishing (CMP), etching, packaging, and so on[3]. Kondo *et al*. showed that at least an 8GPa Young's modulus (E) is required for the porous dielectric to prevent CMP induced damage, especially cracking and delimitation[4]. To obtain these required mechanical properties, the pores' shape and distribution must be strictly controlled to avoid agglomeration and coalescence[5]. A kind of two-dimensional (2D) hexagonal periodic porous silica film with Young's modulus E = 8GPa and k = 2 has been successfully developed as scalable ultra-low-k dielectric by a self-assembled technique[6].

The ability to measure the on-wafer properties of the porous thin films is also needed to predict the successful processing conditions[7]. The surface acoustic wave (SAW) technique is an accurate and nondestructive method available for determining the mechanical properties of different materials. Several experiment results indicate that the Young's modulus of porous low-k films can be evaluated successfully[8~10]. This technique is based on the following characteristic of SAW waves: when propagating in the film-on-substrate layered structure, SAW waves concentrate at the film surface and decay away dependent of the frequency. The SAW velocity versus frequency dispersion relation contains information about mechanical properties of the film[11]. The fitting of theoretical dispersion relations to experimental ones allows the film properties to be measured. Therefore, the measuring accuracy is strongly dependent on the veracity of model used in the theoretical analysis. For computational simplicity, the

* Project supported by the National Natural Science Foundation of China (No. 60406003) and the Scientific Research Foundation for the Returned Overseas Chinese Scholars of the Ministry of Education of China

† Corresponding author. Email: xiaxiao@tju.edu.cn

Received 6 November 2006, revised manuscript received 5 July 2007

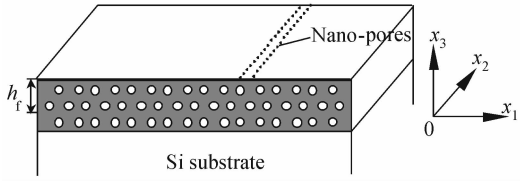

Fig. 1　Schematic diagram of the periodic porous film on Si substrate structure

previous theoretical models treat low-k films as isotropic structures, meaning that only overall effective Young's moduli can be evaluated[11~14]. However, the isotropic model cannot describe the real structure of the periodic porous low-k film. To distinguish the mechanical properties parallel and perpendicular to the pores' direction, a transversely isotropic model is constructed in this paper. The theoretical equations to obtain dispersion curves of SAW waves propagating in this model are given. The effects of Young's moduli, shear modulus of the low-k films on the dispersive characteristics are shown in the numerical examples.

2　Theoretical model

2.1　Anisotropic characters of 2D periodic porous materials

The schematic diagram of the 2D periodic porous film deposited on Si substrate structure is shown in Fig. 1. An orthogonal Cartesian system x_i is set up with its origin located at the interface between the film and substrate. The thickness of the substrate is far more than that of the film h_f, and can be regarded as infinite.

The identical cylindrical pores are along the x_2 direction and hexagonal periodic are distributed in the x_1-x_3 plane, as shown in Fig. 2. The pore diameter is d and the unit cell length is x. Thus, the porosity of the film is defined as[15]

$$P = \frac{\pi d^2}{2\sqrt{3}x^2} \tag{1}$$

The SAW waves are usually generated by thermoelastic absorption of the third-harmonic light pulses of the laser. The elastic displacements and stresses caused by SAW waves are within the region at a depth of approximately one wavelength below the surface. According to the generalized Hooke's law, the stress and the strain have the following linear relation:

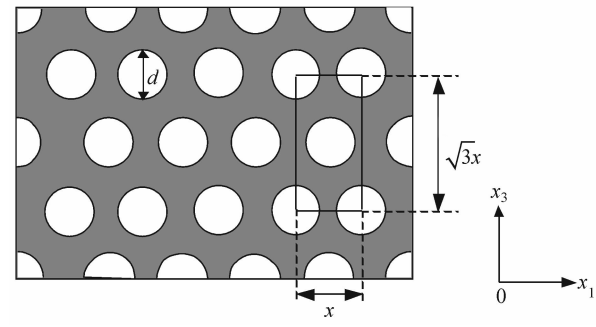

Fig. 2　Schematic diagram of the distribution of nano-pores in the periodic porous film

$$T_{ij} = c_{ijkl}\varepsilon_{kl}, \quad i,j,k,l = 1,2,3 \tag{2}$$

Here c_{ijkl} are the elastic stiffness constants. The independent components of c_{ijkl} are decided by the symmetry of the materials. The most general form of material has 21 independent stiffness components.

In an isotropic solid, there is no directionality and only two independent elastic constants:

$$\begin{aligned} c_{11} &= c_{22} = c_{33} = \frac{E(1-\sigma)}{(1+\sigma)(1-2\sigma)} \\ c_{12} &= c_{23} = c_{31} = \frac{Ev}{(1+\sigma)(1-2\sigma)} \\ c_{44} &= c_{55} = c_{66} = \frac{E}{2(1+\sigma)} \end{aligned} \tag{3}$$

Here E and σ are the Young's modulus and Poisson's ratio of the material, respectively. If the large numbers of nano-pores are uniformly and randomly distributed in the film, this porous film can be considered an isotropic structure. The E and σ of the porous film can be measured by using the isotropic theoretical model.

For the 2D periodic porous film shown in Fig. 1, the nano-pores direction constitutes a principle material direction and perpendicular to this direction is the isotropic plane. Thus, the 2D periodic porous film has a transversely isotropic structure in which the symmetry axis is x_2 and the transversely isotropic plane is parallel to the x_1-x_3 plane. There are five independent components of $\hat{c}_{ijkl}$:

$$\hat{C} = \begin{bmatrix} \hat{c}_{11} & \hat{c}_{12} & \hat{c}_{13} & 0 & 0 & 0 \\ \hat{c}_{12} & \hat{c}_{22} & \hat{c}_{12} & 0 & 0 & 0 \\ \hat{c}_{13} & c_{12} & \hat{c}_{11} & 0 & 0 & 0 \\ 0 & 0 & 0 & \hat{c}_{44} & 0 & 0 \\ 0 & 0 & 0 & 0 & \dfrac{\hat{c}_{11}-\hat{c}_{13}}{2} & 0 \\ 0 & 0 & 0 & 0 & 0 & \hat{c}_{44} \end{bmatrix} \tag{4}$$

Engineering constants for materials, including Young's moduli, Poisson's ratios, and shear moduli have direct physical interpretations. There are five independent engineering constants of a transversely isotropic film: the Young's modulus (E), Poisson's ratio (σ) in the isotropic plane, and the Young's modulus (E'), Poisson's ratio (σ') and shear modulus (G') along the nano-pores' direction. The relationship between the elastic stiffness and corresponding engineering constants are[16]:

$$\hat{c}_{11} = \frac{1-\sigma'^2}{EE'\Delta}, \hat{c}_{12} = \frac{\sigma'(1+\sigma)}{E^2\Delta}, \hat{c}_{13} = \frac{\sigma+\sigma'^2}{EE'\Delta},$$
$$\hat{c}_{22} = \frac{1-\sigma^2}{E^2\Delta}, \hat{c}_{44} = G' \tag{5}$$

where $\Delta = \dfrac{(1+\sigma)(1-\sigma-2\sigma'^2)}{E^2E'}$.

The engineering constants of transversely isotropic porous film have a direct relationship with the porosity, pore diameter, and its distribution. Because of the complexity of the nano-pores distribution in the film, the theoretical and experiential formulas usually take the porosity as variable to predict the engineering constants[17~19]. Eiichi *et al*.[20] measured the pore size of low-k spin-on-glass films using different methods of nondestructive instrumentation. They found that the pore size and spread were increased with increasing porosity, and the porosity could be used as a representative measure of pore size distribution. For the 2D periodic porous film, the relationship between pore size and pore density with the porosity is revealed in Eq. (1). The effects of the pore size and its distribution on the engineering constants can be represented by the porosity change.

2.2 SAW waves propagation in layered structure

When SAW waves propagate in this layered structure, the frequency (f) dependent SAW velocity (v) is determined by the propagation directions ($\boldsymbol{l} = (l_1, l_2, l_3)$) and the physical properties of the film and substrate[10,12]:

$$v = \varphi(f, \boldsymbol{l}, (\hat{c}_{ijkl}, \rho_f, h_f)_{film}, (c_{ijkl}, \rho_s)_{substrate}) \tag{6}$$

where ρ_f and ρ_s are the density of the film and the substrate, respectively, and $\hat{c}_{ijkl}$ and c_{ijkl} are the elastic constants of the film and the substrate, respectively.

The velocity of the plane wave propagating in an anisotropic medium is given by the Christoffel equation:

$$[\Gamma_{jk} - \rho v^2 \delta_{jk}]\alpha_k = 0 \tag{7}$$

Here $\Gamma_{jk} = l_i l_l c_{ijkl}$ is the Christoffel stiffness. The Christoffel stiffness of 2D periodic porous film $\hat{\Gamma}_{ijkl}$ and cubic Si Γ_{ijkl} are:

$$\begin{cases}
\hat{\Gamma}_{11} = l_1^2 \hat{c}_{11} + l_2^2 \hat{c}_{44} + (l_3+b)^2 \hat{c}_{55} \\
\hat{\Gamma}_{12} = l_1 l_2 (\hat{c}_{12} + \hat{c}_{44}) \\
\hat{\Gamma}_{13} = l_1 (l_3+b)(\hat{c}_{13} + \hat{c}_{55}) \\
\hat{\Gamma}_{21} = \Gamma_{12} \\
\hat{\Gamma}_{22} = l_1^2 \hat{c}_{44} + l_2^2 \hat{c}_{22} + (l_3+b)^2 \hat{c}_{44} \\
\hat{\Gamma}_{23} = l_2 (l_3+b)(\hat{c}_{12} + \hat{c}_{44}) \\
\hat{\Gamma}_{31} = \Gamma_{13} \\
\hat{\Gamma}_{32} = \Gamma_{23} \\
\hat{\Gamma}_{33} = l_1^2 \hat{c}_{55} + l_2^2 \hat{c}_{44} + (l_3+b)^2 \hat{c}_{11}
\end{cases} \tag{8}$$

$$\begin{cases}
\Gamma_{11} = l_1^2 c_{11} + l_2^2 c_{44} + (l_3+b)^2 c_{44} \\
\Gamma_{12} = l_1 l_2 c_{12} + l_1 l_2 c_{44} \\
\Gamma_{13} = l_1 (l_3+b)(c_{12} + c_{44}) \\
\Gamma_{21} = \Gamma_{12} \\
\Gamma_{22} = l_1^2 c_{44} + l_2^2 c_{11} + (l_3+b)^2 c_{44} \\
\Gamma_{23} = l_2 (l_3+b)(c_{12} + c_{44}) \\
\Gamma_{31} = \Gamma_{13} \\
\Gamma_{32} = \Gamma_{23}
\end{cases} \tag{9}$$

If a propagating plane wave in a medium is interrupted by a boundary, certain conditions must be satisfied at that boundary. For the porous film on substrate structure with two boundaries, the interface ($x_3 = 0$) and the free surface ($x_3 = h_f$) boundary conditions include:

(1) Continuity of the displacement at the interface ($x_3 = 0$):

$$\hat{u}_1 = u_1, \hat{u}_2 = u_2, \hat{u}_3 = u_3 \tag{10}$$

(2) Continuity of the stress at the interface ($x_3 = 0$):

$$\hat{T}_{31} = T_{31}, \hat{T}_{32} = T_{32}, \hat{T}_{33} = T_{33} \tag{11}$$

(3) Vanishing of the stress at the free surface ($x_3 = h_f$):

$$\hat{T}_{31} = 0, \hat{T}_{32} = 0, \hat{T}_{33} = 0 \tag{12}$$

where $\hat{u}_j$ and u_j are the particle displacements in the film and substrate, respectively:

$$\hat{u}_i = \sum_n C_n \alpha_i^{(n)} \exp(ikb^{(n)} x_3) \exp[ik(l_1 x_1 + l_2 x_2 + l_3 x_3 - vt)], \quad n = 1,2,3,4,5,6 \tag{13}$$

$$u_i = \sum_m C_m \alpha_i^{(m)} \exp(ikb^{(m)} x_3) \exp[ik(l_1 x_1 + l_2 x_2 + l_3 x_3 - vt)], \quad m = a,c,d \tag{14}$$

where $\hat{T}_{3j}$ and T_{3j} are the traction components of the stress in the film and substrate, respectively:

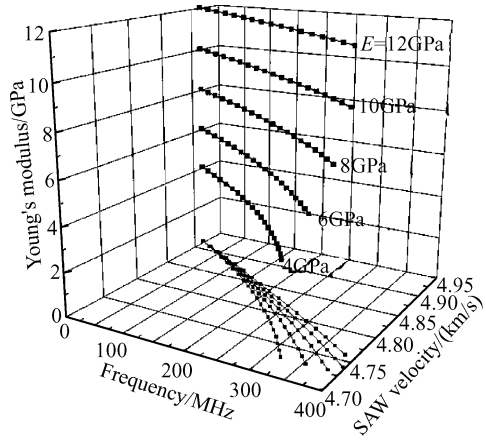

Fig. 3　3D dispersive curves and their projections when propagating along the [100] direction　Young's modulus E changes from 4 to 12GPa.

$$\hat{T}_{3j} = \hat{c}_{3jil}\frac{\partial \hat{u}_i}{\partial x_l}, \quad T_{3j} = c_{3jil}\frac{\partial u_i}{\partial x_l} \tag{15}$$

Substituting Eqs. (13～15) into Eqs. (10～12), we get:

$$M \times [C_1 \quad C_2 \quad C_3 \quad C_4 \quad C_5 \quad C_6 \quad C_c \quad C_d \quad C_e]' = 0 \tag{16}$$

M is a 9×9 boundary conditions matrix. Solving the secular equation of M gives the propagation vector k, and thus we acquire the dispersive relationship between the frequency and SAW velocity according to $f = kv/2\pi$. Given the different mechanical properties of the film as parameters, a series of dispersive curves can be made.

3　Numerical examples

In the following computations, the SAW waves are assumed to propagate along the [100] direction, whose direction cosines are $l_1 = 1$, $l_2 = 0$ and $l_3 = 0$, and the [110] direction, whose direction cosines are $l_1 = \frac{\sqrt{2}}{2}$, $l_2 = \frac{\sqrt{2}}{2}$ and $l_3 = 0$, respectively.

The density (ρ_f) and thickness (h_f) of the film are set to 1.0g/cm^3 and 600nm, respectively. To ensure the validity of the numerical examples, the engineering constants of periodic porous low-k film adopt the theoretical prediction results given by Hashin and Bert. When the porosity is 77%, the engineering constants approximate to: $E = 8$GPa, $\sigma = 0.33$, $E' = 16$GPa, $\sigma' = 0.18$, $G' = 4$GPa.

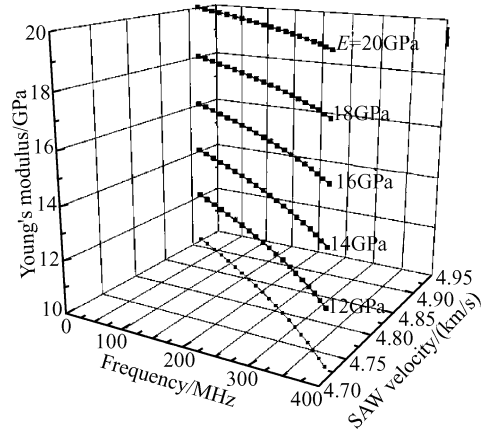

Fig. 4　3D dispersive curves and their projections when propagating along the [100] direction　Young's modulus E' changes from 12 to 20GPa.

The density and elastic constants of Si (100) substrate are $\rho_s = 2.330$g/cm^3, $c_{11} = 165.7$GPa, $c_{12} = 63.9$GPa, $c_{44} = 79.6$GPa, respectively.

Figure 3 shows the three-dimensional (3D) dispersive curves when the SAW propagation direction is [100] and the Young's modulus E changes from 4 to 12GPa. In the low frequency area, the SAW velocity value corresponds to the pseudo-surface wave (PSW) in the [100] direction of the Si (100) surface, that is 4.917km/s. As the frequency increases, the SAW velocity decreases continually because the film is softer than the substrate. And the smaller the Young's modulus E is, the faster the velocity decreases.

Figures 4 and 5 show the 3D dispersive curves in the [100] direction when the Young's modulus

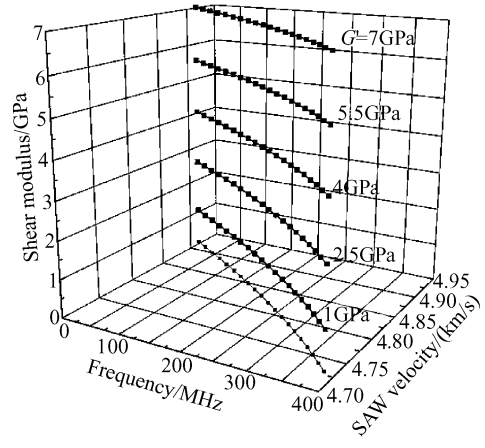

Fig. 5　3D dispersive curves and their projections when propagating along the [100] direction　Shear modulus G' changes from 1 to 7GPa.

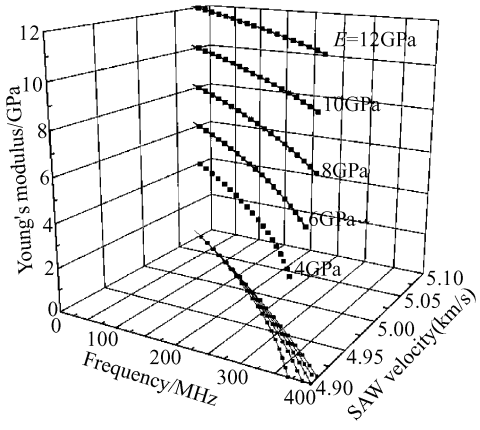

Fig. 6 3D dispersive curves and their projections when propagating along the [110] direction Young's modulus E changes from 4 to 12GPa.

E' and shear modulus G' change. Compared to the curves in Fig. 3, the SAW velocity decreases continually with the increase of frequency, but does not change when either the E' or the G' varies. The projection curves in the SAW velocity-frequency plane are superposed, and indicate that when the SAW waves propagate perpendicular in the direction of the nano-pores, the mechanical properties along the direction of nano-pores do not affect the dispersive curves. These dispersive characteristics reveal that E' and G' cannot be measured when the SAW waves propagate along the [100] direction.

The main reason for this phenomenon is that the particle displacements caused by the SAW waves have only two components, one of which is parallel to the propagation direction and of which the other is perpendicular to the free surface of the solid film[21]. When the SAW waves propagate along the [100] direction, the particle displacements have no components perpendicular to the propagation direction. The engineering constants along the symmetry axes E', σ' and G' do not affect the propagation of SAW waves.

Figures 6～8 show the 3D dispersive curves in the [110] direction when the Young's modulus E, Young's modulus E', and shear modulus G' change. In the low frequency area, the SAW velocity value corresponds to the PSW in the [110] direction of the Si (100) surface, that is 5.082km/s. The curvatures of the dispersive curves will become larger with the increase of frequency when any of the moduli E, E' or G' decreases. And the smaller the moduli are, the larger the curvatures are. Each dispersive curve includes the information of a set of E, E' and G'. These dispersive characteristics indicate that all these moduli can be measured when the SAW waves propagate along the [110] direction. Maznev successfully measured four elastic constants of transversely isotropic mesoporous materials by using a laser-generated SAWs technique[22].

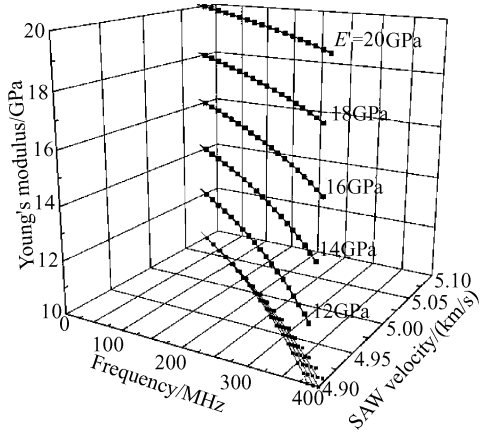

Fig. 7 3D dispersive curves and their projections when propagating along the [110] direction Young's modulus E' changes from 12 to 20GPa.

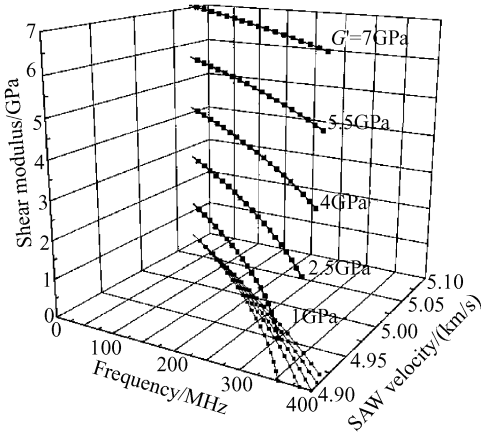

Fig. 8 3D dispersive curves and their projections when propagating along the [110] direction Shear modulus G' changes from 1 to 7GPa.

The following methods are beneficial to improve the fitting accuracy in the experiments:

(1) To measure the density and thickness of the porous film by other methods, such as X-ray reflectance and spectroscopic ellipsometry, so that they can be used as known parameters for theoretical calculation.

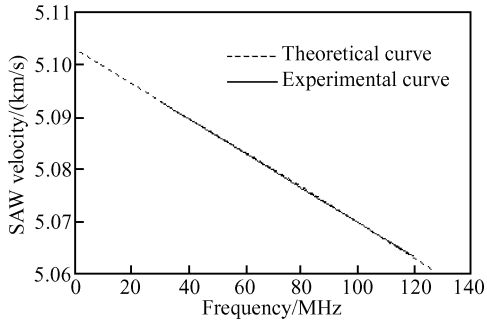

Fig. 9　Elastic moduli determination for periodic porous silica

(2) The alignment accuracy of propagation direction can be improved by using a twin-transducer[23].

(3) Measuring in several different propagation directions will produce different dispersive curves. The unknown parameters can be decided by repeatedly fitting these experimental curves with those theoretical ones.

(4) Because the larger dispersion curvature in the higher frequencies can distinguish one curve from the others, raising the frequency detection broadband of the SAW detection in the experiments more than 300MHz will remarkably improve the curves' fitting accuracy.

Mechanical properties of periodic porous silica were measured by laser-generated SAW technique as shown in Fig. 9. Periodic porous silica thin films were developed by spin-coating at 2000 ~6000r/min on a p-type Si (100) substrate by a sol-gel process. The film density 1.15g/cm^3 and thickness 186nm were determined accurately by X-ray reflectance and spectroscopic ellipsometry. The measured elastic moduli are E = 1.1GPa, E' = 2.1GPa, G' = 0.3GPa.

4　Conclusions

A new propagation model for the SAW measurement of periodic porous low-k materials has been present in detail. Structural change of low-k film caused by the introduction of nano-pores has been taken into account in this model. From numerical examples, the dispersive characteristics of SAW waves propagating in the layered structure of transversely isotropic porous film deposited on Si (100) substrate has been expressed. It has been demonstrated that all the Young's moduli E, E' and shear modulus G' can be measured when the propagation direction of SAW waves is not perpendicular to the direction of the nano-pores. The model and results can instruct the experiments of mechanical properties determination of 2D periodic porous low-k film by SAW measurement.

References

[1] http://www.itrs.net/Links/2005ITRS/Home2005.htm
[2] Jain A, Rogojevic S, Ponoth S, et al. Porous silica materials as low-k dielectrics for electronic and optical interconnects. Thin Solid Films, 2001, 398/399: 513
[3] Jin C, Lin S, Wetzel J T. Evaluation of ultra-low-k dielectric materials for advanced interconnects. J Electron Mater, 2001, 30(4): 284
[4] Kondo S, Tokitoh S, Yoon B U, et al. Low-pressure CMP for reliable porous low-k/Cu integration. Proceedings of IITC, 2003: 86
[5] Treichel H. Low dielectric constant materials. J Electron Mater, 2001, 30(4): 290
[6] Kikkawa T, Oku Y, Kohmura K, et al. A scalable low-k/Cu interconnect technology using self-assembled ultra-low-k porous silica films. 7th ICSICT, 2004, 1~3: 493
[7] Bauer B J, Lin E K, Lee H J, et al. Structure and property characterization of low-k dielectric porous thin films. J Electron Mater, 2001, 30(4): 304
[8] Flannery C M, Murray C, Sueiter I, et al. Characterization of thin-film aerogel porosity and stiffness with laser-generated surface acoustic waves. Thin Solid Films, 2001, 388: 1
[9] Schneider D, Siemroth P, Schulke T, et al. Quality control of ultra-thin and super-hard coatings by laser-acoustics. Surf Coat Tech, 2002, 153(2): 252
[10] Xiao X, Hata N, Yamada K, et al. Mechanical properties of periodic porous silica low-k films determined by the twin-transducer surface acoustic wave technique. Rev Sci Instrum, 2003, 10: 4539
[11] Farnell G W, Adler E L. Physical acoustics. New York, London: Academic Press, 1972, 9: 35
[12] Li Zhiguo, Xiao Xia, Zhang Xinhui, et al. Dispersive characteristics of surface acoustic waves for measuring mechanical properties of low-k dielectrics used in ULSI. Chinese Journal of Semiconductors, 2005, 26(10): 2032 (in Chinese) [李志国, 肖夏, 张鑫慧, 等. 表征 ULSI 低介电常数互连材料机械特性的表面波频散特性. 半导体学报, 2005, 26(10): 2032]
[13] Schneider D, Schwarz T, Schultrich B. Determination of elastic modulus and thickness of surface layers by ultrasonic surface waves. Thin Solid Films, 1992, 219: 92
[14] Xiao Xia, You Xueyi. Numerical study on surface acoustic wave method for determining Young's modulus of low-k films involved in multi-layered structures. Appl Surf Sci, 2006, 253: 2958
[15] Hidenori M, Hisanori M, Hrofumi T, et al. Theoretical investigation of dielectric constant and elastic modulus of two-dimensional periodic porous silica films with elliptical cylindrical pores. Jpn J Appl Phys, 2005, 44(3): 1161
[16] Brain M L. Ultrasound and elastic waves frequently asked questions. New York, London: Academic Press, 2002
[17] Hashin Z, Rosen B W. The elastic moduli of fiber-reinforced

materials. J Appl Mechanics, 1964, 31(2): 223
[18] Bert C W. Prediction of elastic moduli of solids with oriented porosity. J Mater Sci, 1985, 20: 2220
[19] Herakovich C T, Baxter S C. Influence of pore geometry on the effective response of porous media. J Mater Sci, 1999, 34: 1595
[20] Eiichi K, Mikhail R B, Eric L, et al. Comparative study of pore size of low-dielectric-constant spin-on-glass films using different methods of nondestructive instrumentation. Jpn J Appl Phys, 2001, 40: L323
[21] Rose J L. Ultrasonic waves in solid media. Cambridge University Press, 1999
[22] Manev A A, Mazurenko A, Alper G, et al. Anisotropic elastic properties of low-k dielectric materials, technology and reliability for advanced interconnects and low-k dielectrics. MRS Proceedings, 2004, 812: F5.9
[23] Xiao Xia, Zhang Xinhui, Yao Suying. Alignment technique used in the SAW method for characterizing the mechanical property of the nano-porous SiO_2. Nanotechnology and Precision Engineering, 2005, 3(2): 122 (in Chinese) [肖夏, 张鑫慧, 姚素英. 表面波方法表征纳米多孔 SiO_2 薄膜机械特性的对准技术. 纳米技术与精密工程, 2005, 3(2): 122]

周期性多孔低介电常数材料机械特性的表面波测量模型*

李志国 姚素英 肖 夏† 白茂森

(天津大学电子信息工程学院 专用集成电路设计中心，天津 300072)

摘要：研究了纳米通孔的分布对于表面波方法测量多孔低介电常数薄膜机械特性的影响，提出了用横观各向同性表征周期性多孔介质材料结构特性的表面波传播理论模型，给出了表面波在 low-k 薄膜/Si 基底分层结构中的传播方程. 通过数值算例揭示出表面波在不同传播方向的频散特性，以及 low-k 薄膜的弹性常数即杨氏模量 E，E' 和剪切模量 G' 对频散特性的影响. 结果表明 E' 和 G' 在垂直于通孔的传播方向不能被测出.

关键词：周期性多孔材料；低介电常数介质；横观各向同性对称；机械特性；表面波测量

PACC：0340K；0630M；6860 **EEACC**：2570；2800；7320G

中图分类号：TN405.97 **文献标识码**：A **文章编号**：0253-4177(2007)11-1722-07

* 国家自然科学基金(批准号：60406003)和教育部留学回国人员科研启动基金资助项目

† 通信作者. Email: xiaxiao@tju.edu.cn

2006-11-06 收到，2007-07-05 定稿